

A test of *psbK-psbI* and *atpF-atpH* as potential plant DNA barcodes using the flora of the Kruger National Park as a model system (South Africa)

Renaud Lahaye^{1,*}, Vincent Savolainen^{2,3}, Sylvie Duthoit¹, Olivier Maurin¹ and Michelle van der Bank¹

Author affiliation: ¹Department of Botany and Plant Biotechnology, APK Campus, University of Johannesburg, P. O. Box 524, Auckland Park 2006, Johannesburg, South Africa; ²Royal Botanic Gardens, Kew, Richmond TW9 3DS, UK; ³Imperial College London, Silwood Park Campus, Buckhurst Road, Ascot SL5 7PY, UK.

We thank the South African National Research Foundation, the University of Johannesburg, SASOL, the UK Darwin Initiative, and The Royal Society (UK) for funding. We also thank the Kruger National Park, South African National Parks, H. Eckhardt, I. Smit, G. Zambatis, T. Khosa, for granting access to the park and sharing data; Stephen Boatwright for proofreading the manuscript; and T. Rikombe, R. Bryden, T. Mhlongo, H. van der Bank for fieldwork.

***To whom correspondence should be addressed:** lahaye@cict.fr

Introduction

DNA barcoding is a new technique that uses short, standardized DNA sequences (400-800 bp) of an organism to determine its identity. Because this sequence has to be variable enough to identify individual species, but not too variable within the same species so that a clear threshold can be defined between intra- and inter-specific diversities, it is very challenging to apply this technique to all species on the planet. A DNA barcode has been identified for animals, i.e. the mitochondrial gene *cox1*, which shows strong abilities in identifying cryptic species, accelerating biodiversity inventories and helping to identify species from degraded material (e.g. to control trade of threatened). For plants, the identification of a suitable DNA barcode is more problematic. Cho et al. showed that mitochondrial DNA evolves too slowly in plants to provide a region variable enough to discriminate between species. Then the quest for the best suitable barcode started and is still ongoing.

Kress et al. opened the debates and suggested the use of multiple genes to identify plant species quickly and accurately. At the Second International Barcode of Life Conference in Taipei (September 2007), at least five different plant DNA barcodes were proposed, but no consensus reached. Among those, both *atpF-atpH* and *psbK-psbI* suggested by Kim et al. have not yet been tested. Here, we evaluate the use of these loci as DNA barcodes for plants by applying them to a wide range of plant species. The two new intergenic loci *atpF-atpH* and *psbK-psbL* are both localized in the large single copy (LSC) of the plastid genome. The genes *atpF* and *atpH* encode ATP synthase subunits CFO I and CFO III, respectively. Both genes *psbK* and *psbI* encode two low molecular mass polypeptides, K and I, respectively, of the photo-system II. These two new loci are conservative from algae to land plants and even in parasitic plants. In this study, we focus on the trees and shrubs from the Kruger National Park (hereafter KNP), part of the Maputaland-Pondoland-Albany hotspot in southern Africa. On a selected sampling from

the 2,700 taxa surveyed in the area, we applied several metrics following Lahaye et al. to evaluate the efficiency of combining *matK* either to *trnH-psbA* and/or *atpF-atpH* and/or *psbK-psbI* for DNA barcoding purposes.

Material and Methods

Sampling. In total 101 taxa from the KNP were sampled, covering 18 families from the monocotyledons to the euasterids II. This dataset included 31 species of trees and shrubs in which we had more than one representative per species, 3 species of Orchids, one of which with 2 representatives, and 3 parasitic plants, one of which is achlorophyllous. Parasitic plants have been sampled to test the universality of the potential DNA barcodes. We used *Amborella trichopoda* Baill. (complete genome GenBank accession AJ506156) as outgroup for the phylogenetic analyses. All specimens were collected in different ecosystems when possible (Figure 1) and voucher specimens are available as detailed in Table 1.

Collection and preservation. Collection of plant material was done in the KNP with the assistance of the park's rangers. Plants were sampled and pressed for herbarium voucher specimens in triplicate, one for the herbarium of the KNP, one for Kew Herbarium (K; United Kingdom), and one for the herbarium at Pretoria (PRE; South Africa). Information about the locality and habit of collected plants were entered on a palmtop-GPS to facilitate their further treatment, and also noted on hard copy for security. For each plant collected, leaf material was stored in silica for molecular studies, and flowers and fruit stored in ethanol when available.

DNA sequencing. Total DNA was extracted from dried leaf material using the standard method of Doyle and Doyle and cleaned with QIAquick silica columns (Qiagen, Helden,

Germany). Sequences of *matK* and *trnH-psbA* for each taxa were published in Lahaye et al. and their accession numbers are available from GenBank (Table 1). We amplified *atpF-atpH* and *psbK-psbI* using PCR as follows: 35 cycles, 30 sec denaturation at 94°C, 40 sec annealing at 51°C, and 40 sec extension at 72°C. Primers were kindly provided by Kim Ki-Joong: *atpF-atpH*: *atpF* 5'-ACTCGCACACACTCCCTTTCC-3', *atpH* 5'-GCTTTTATGGAAGCTTTAACAAT-3'; and *psbK-psbI*: *psbK*-5'-TTAGCCTTTGTTTGGCAAG-3', *psbI*-5'-AGAGTTTGAGAGTAAGCAT-3'. After cycle sequencing using Big Dye terminator v3.1 and sequencing on a 3130xl genetic analyzer (Applied Biosystems, UK), electropherograms were edited using SEQUENCER 4.6 software (Genes Codes Corporation, USA) and DNA sequences aligned by eye in PAUP4b10* (incomplete sequences at both ends were excluded from the analyses). Taxa with missing data (amplification or sequencing failed) were removed from the combined matrix in order to analyze complete matrices.

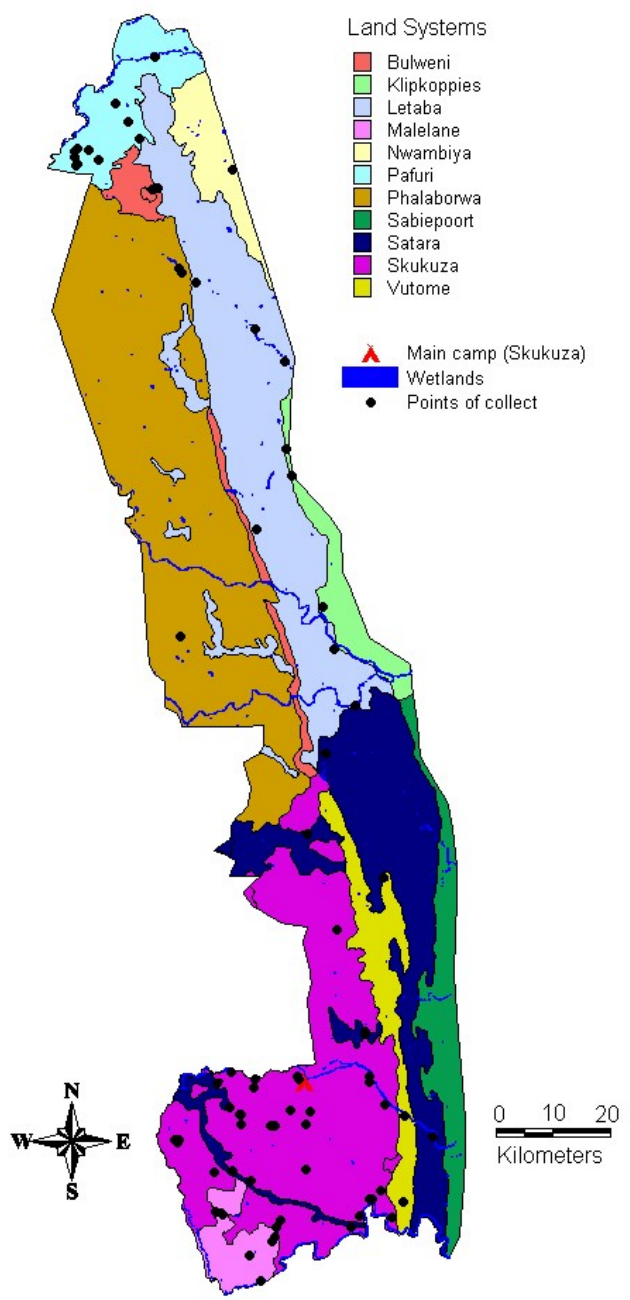


Figure 1. Map of the KNP with landsystems following Venter (1990) and collecting points from this study

| Plant Family | name Checked on IPNI | Voucher | Location | GPS | Altitude | matK | trnH-psbA | atpF-atpH | psbK-psbI |
|---------------|---|---------|----------|-------------------------|----------|----------|-----------|-----------|-----------|
| Fabaceae | <i>Acacia exuvialis</i> Verdoorn | OM260 | KNP | S24 58 54.3 E31 34 26.3 | 284 m | EU214205 | EU213781 | - | EU626889 |
| Fabaceae | <i>Acacia exuvialis</i> Verdoorn | RL1204 | KNP | S25 29 35.4 E31 28 12.3 | 319 m | EU214206 | EU213782 | EU626796 | EU626890 |
| Fabaceae | <i>Acacia exuvialis</i> Verdoorn | RL1412 | KNP | S25 21 41.5 E31 30 56.5 | 320 m | EU214207 | EU213783 | - | EU626891 |
| Fabaceae | <i>Acacia nigrescens</i> Oliver | RL1111 | KNP | S25 06 26.4 E31 30 24.5 | 452 m | EU214208 | - | EU626797 | EU626892 |
| Fabaceae | <i>Acacia nigrescens</i> Oliver | RL1205 | KNP | S25 29 35.4 E31 28 12.3 | 319 m | EU214209 | EU213784 | EU626798 | EU626893 |
| Fabaceae | <i>Acacia nigrescens</i> Oliver | RL1656 | KNP | S22 41 29.6 E31 01 37.2 | 439 m | EU214210 | EU213785 | EU626799 | EU626894 |
| Fabaceae | <i>Acacia tortilis</i> Hayne | OM261 | KNP | S24 59 20.9 E31 34 34.5 | 266 m | EU214213 | EU213788 | EU626800 | EU626895 |
| Fabaceae | <i>Acacia tortilis</i> Hayne | RL1483 | KNP | S24 36 53.6 E31 40 51.4 | 333 m | EU214211 | EU213786 | EU626801 | EU626896 |
| Fabaceae | <i>Acacia tortilis</i> Hayne | RL1608 | KNP | S22 57 38.1 E31 14 50.5 | 302 m | EU214212 | EU213787 | EU626802 | EU626897 |
| Orchidaceae | <i>Acampe praemorsa</i> (Roxb.) Blatt. & McCann | RBN203 | KNP | S22 42 06.1 E30 58 14.4 | 504 m | EU214214 | EU213789 | EU626803 | EU626898 |
| Amborellaceae | <i>Amborella trichopoda</i> Baill. | - | - | - | - | AJ506156 | AJ506156 | AJ506156 | AJ506156 |
| Orchidaceae | <i>Ansellia africana</i> Lindl. | OM1163 | KNP | S25 12 54.8 E31 35 36.0 | 280 m | EU214215 | - | EU626804 | EU626899 |
| Orchidaceae | <i>Ansellia africana</i> Lindl. | OM531 | KNP | S25 19 54.3 E31 44 28.5 | 225 m | EU214216 | - | EU626805 | EU626900 |
| Orchidaceae | <i>Bonatea speciosa</i> Willd. | RL1158 | KNP | S25 13 11.4 E31 23 41.8 | 472 m | EU214217 | EU213790 | EU626806 | EU626901 |
| Asteraceae | <i>Brachylaena huillensis</i> O.Hoffm. | OM1281 | KNP | S23 28 54.6 E31 33 27.0 | 421 m | EU214218 | EU213791 | EU626807 | EU626902 |
| Asteraceae | <i>Brachylaena huillensis</i> O.Hoffm. | OM247 | KNP | S25 06 12.7 E31 35 44.2 | 276 m | EU214219 | EU213792 | EU626808 | EU626903 |
| Asteraceae | <i>Brachylaena huillensis</i> O.Hoffm. | RBN360 | KNP | S22 42 51.4 E31 23 46.3 | 507 m | EU214220 | EU213793 | EU626809 | EU626904 |
| Combretaceae | <i>Combretum apiculatum</i> Sond. | RL1100 | KNP | S25 06 24.7 E31 30 41.4 | 389 m | EU214221 | EU213794 | EU626810 | EU626905 |
| Combretaceae | <i>Combretum apiculatum</i> Sond. | RL1185 | KNP | S25 23 11.2 E31 30 42.1 | 391 m | EU214222 | EU213795 | EU626811 | EU626906 |
| Combretaceae | <i>Combretum apiculatum</i> Sond. | RL1355 | KNP | S25 20 11.4 E31 49 48.0 | 213 m | EU214223 | EU213796 | EU626812 | EU626907 |
| Combretaceae | <i>Combretum collinum</i> Fresen. | OM722 | KNP | S25 00 07.4 E31 21 07.0 | 378 m | EU214224 | EU213797 | EU626813 | EU626908 |
| Combretaceae | <i>Combretum collinum</i> Fresen. | RL1164 | KNP | S25 14 44.5 E31 26 39.8 | 419 m | EU214225 | EU213798 | EU626814 | EU626909 |
| Combretaceae | <i>Combretum collinum</i> Fresen. | RL1392 | KNP | S25 25 45.2 E31 26 26.4 | 334 m | EU214226 | EU213799 | EU626815 | EU626910 |
| Combretaceae | <i>Combretum hereroense</i> Schinz | RL1120 | KNP | S25 06 28.6 E31 29 58.5 | 383 m | EU214227 | EU213800 | EU626816 | EU626911 |
| Combretaceae | <i>Combretum hereroense</i> Schinz | RL1183 | KNP | S25 23 11.2 E31 30 42.1 | 391 m | EU214228 | EU213801 | EU626817 | EU626912 |
| Combretaceae | <i>Combretum hereroense</i> Schinz | RL1364 | KNP | S25 17 18.5 E31 46 34.6 | 235 m | EU214229 | EU213802 | EU626818 | EU626913 |
| Euphorbiaceae | <i>Croton gratissimus</i> Burch | OM785 | KNP | S23 48 24.9 E31 38 27.2 | 285 m | EU214230 | EU213803 | EU626819 | EU626914 |
| Euphorbiaceae | <i>Croton gratissimus</i> Burch | RL1619 | KNP | S22 45 43.6 E31 10 50.8 | 379 m | EU214231 | EU213804 | EU626820 | EU626915 |
| Euphorbiaceae | <i>Croton gratissimus</i> Burch | RL1621 | KNP | S22 45 52.1 E31 10 29.1 | 414 m | EU214232 | EU213805 | EU626821 | EU626916 |

| Plant Family | name Checked on IPNI | Voucher | Location | GPS | Altitude | matK | trnH-psbA | atpF-atpH | psbK-psbI |
|---------------|--|---------|----------|-------------------------|----------|----------|-----------|-----------|-----------|
| Euphorbiaceae | <i>Croton megalobotrys</i> Müll.Arg. | OM774 | KNP | S24 03 13.4 E31 43 50.0 | 211 m | EU214233 | EU213806 | EU626822 | EU626917 |
| Euphorbiaceae | <i>Croton megalobotrys</i> Müll.Arg. | RL1540 | KNP | S23 54 53.6 E31 40 18.7 | 201 m | EU214234 | EU213807 | EU626823 | EU626918 |
| Euphorbiaceae | <i>Croton megalobotrys</i> Müll.Arg. | RL1574 | KNP | S23 11 37.5 E31 32 16.5 | 246 m | EU214235 | EU213808 | EU626824 | EU626919 |
| Euphorbiaceae | <i>Croton pseudopulchellus</i> Pax | RBN186 | KNP | S22 39 57.7 E30 59 57.6 | 468 m | EU214236 | EU213809 | EU626825 | EU626920 |
| Euphorbiaceae | <i>Croton pseudopulchellus</i> Pax | RBN262 | KNP | S22 26 00.7 E31 10 57.6 | 291 m | EU214237 | EU213810 | EU626826 | EU626921 |
| Euphorbiaceae | <i>Croton pseudopulchellus</i> Pax | RL1650 | KNP | S22 40 09.2 E30 57 39.6 | 451 m | EU214238 | EU213811 | - | EU626922 |
| Orchidaceae | <i>Eulophia</i> R.Br. | OM473 | KNP | S25 03 40.0 E31 23 11.2 | 351 m | EU214239 | EU213812 | EU626827 | EU626923 |
| Proteaceae | <i>Faurea rochetiana</i> Chiov. ex Pic.Serm. | OM1413 | KNP | S25 08 43.0 E31 14 33.4 | 726 m | EU214240 | EU213813 | EU626828 | EU626924 |
| Proteaceae | <i>Faurea rochetiana</i> Chiov. ex Pic.Serm. | OM1461 | KNP | S25 08 43.6 E31 14 32.6 | 722 m | EU214241 | EU213814 | EU626829 | EU626925 |
| Proteaceae | <i>Faurea rochetiana</i> Chiov. ex Pic.Serm. | OM1463 | KNP | S25 08 43.1 E31 14 33.1 | 727 m | EU214242 | EU213815 | EU626830 | EU626926 |
| Proteaceae | <i>Faurea saligna</i> Harv. | OM1438 | KNP | S25 19 31.7 E31 21 42.3 | 486 m | EU214243 | EU213816 | EU626831 | EU626927 |
| Proteaceae | <i>Faurea saligna</i> Harv. | OM1443 | KNP | S25 19 16.9 E31 20 59.5 | 523 m | EU214244 | EU213817 | EU626832 | EU626928 |
| Proteaceae | <i>Faurea saligna</i> Harv. | OM1445 | KNP | S25 19 39.5 E31 22 08.8 | 473 m | EU214245 | EU213818 | EU626833 | EU626929 |
| Moraceae | <i>Ficus abutilifolia</i> Miq. | OM557 | KNP | S25 04 41.4 E31 24 54.5 | 414 m | EU214248 | EU213821 | EU626834 | EU626930 |
| Moraceae | <i>Ficus abutilifolia</i> Miq. | RL1471 | KNP | S24 52 32.9 E31 45 21.9 | 256 m | EU214246 | EU213819 | EU626835 | EU626931 |
| Moraceae | <i>Ficus abutilifolia</i> Miq. | RL1501 | KNP | S24 22 39.3 E31 35 51.8 | 369 m | EU214247 | EU213820 | EU626836 | EU626932 |
| Moraceae | <i>Ficus glumosa</i> Delile | OM564 | KNP | S25 04 36.8 E31 25 03.7 | 473 m | EU214249 | EU213822 | EU626837 | EU626933 |
| Moraceae | <i>Ficus glumosa</i> Delile | RL1407 | KNP | S25 23 41.1 E31 30 02.4 | 466 m | EU214250 | EU213823 | EU626838 | EU626934 |
| Moraceae | <i>Ficus glumosa</i> Delile | RL1429 | KNP | S25 08 29.6 E31 14 42.6 | 665 m | EU214251 | EU213824 | EU626839 | - |
| Moraceae | <i>Ficus sycomorus</i> L. | RBN197 | KNP | S22 40 53.4 E30 57 43.2 | 445 m | EU214252 | EU213825 | EU626840 | EU626935 |
| Moraceae | <i>Ficus sycomorus</i> L. | RL1598 | KNP | S23 06 46.1 E31 27 16.5 | 264 m | EU214253 | EU213826 | EU626841 | EU626936 |
| Moraceae | <i>Ficus sycomorus</i> L. | RL1614 | KNP | S22 45 43.1 E31 11 18.4 | 356 m | EU214254 | EU213827 | EU626842 | EU626937 |
| Malvaceae | <i>Grewia bicolor</i> Juss. | OM329 | KNP | S25 04 18.8 E31 36 29.5 | 363 m | EU214255 | EU213828 | EU626843 | EU626938 |
| Malvaceae | <i>Grewia bicolor</i> Juss. | RL1545 | KNP | S23 36 52.2 E31 27 36.5 | 290 m | EU214256 | EU213829 | EU626844 | EU626939 |
| Malvaceae | <i>Grewia bicolor</i> Juss. | RL1658 | KNP | S22 41 29.6 E31 01 37.2 | 439 m | EU214257 | EU213830 | EU626845 | EU626940 |
| Malvaceae | <i>Grewia flavescens</i> Juss. | OM323 | KNP | S25 04 18.8 E31 36 29.5 | 363 m | EU214258 | EU213831 | - | EU626941 |
| Malvaceae | <i>Grewia flavescens</i> Juss. | RL1472 | KNP | S24 52 32.9 E31 45 21.9 | 256 m | EU214259 | EU213832 | EU626846 | EU626942 |
| Malvaceae | <i>Grewia flavescens</i> Juss. | RL1604 | KNP | S22 58 18.8 E31 15 13.5 | 305 m | EU214260 | - | - | - |
| Malvaceae | <i>Grewia villosa</i> Willd. | RL1342 | KNP | S24 58 56.5 E31 46 02.3 | 208 m | EU214261 | EU213833 | - | EU626943 |
| Malvaceae | <i>Grewia villosa</i> Willd. | RL1523 | KNP | S24 10 31.8 E31 38 53.8 | 255 m | EU214262 | EU213834 | EU626847 | EU626944 |

| Plant Family | name Checked on IPNI | Voucher | Location | GPS | Altitude | matK | trnH-psbA | atpF-atpH | psbK-psbI |
|----------------|--|---------|----------|-------------------------|----------|----------|-----------|-----------|-----------|
| Malvaceae | <i>Grewia villosa</i> Willd. | RL1569 | KNP | S23 24 48.9 E31 32 21.8 | 363 m | EU214263 | EU213835 | - | EU626945 |
| Apiaceae | <i>Heteromorpha arborescens</i> Cham. & Schltld. | OM1430 | KNP | S25 13 27.0 E31 20 34.3 | 655 m | EU214264 | EU213836 | EU626848 | EU626946 |
| Apiaceae | <i>Heteromorpha arborescens</i> Cham. & Schltld. | OM1488 | KNP | S24 59 58.3 E31 21 04.3 | 359 m | EU214265 | EU213837 | EU626849 | EU626947 |
| Apiaceae | <i>Heteromorpha arborescens</i> Cham. & Schltld. | OM1516 | KNP | S25 20 29.0 E31 31 25.8 | 426 m | EU214266 | EU213838 | EU626850 | EU626948 |
| Hydnoraceae | <i>Hydnora johannis</i> Becc. | OM534 | KNP | S25 21 37.5 E31 43 11.1 | 241 m | EU214267 | - | - | EU626949 |
| Arecaceae | <i>Hyphaene coriacea</i> Gaertn. | OM1184 | KNP | S25 08 03.4 E31 56 37.7 | 167 m | EU214268 | EU213775 | EU626851 | EU626950 |
| Arecaceae | <i>Hyphaene coriacea</i> Gaertn. | OM1187 | KNP | S25 17 45.4 E31 51 44.5 | 185 m | EU214269 | EU213776 | EU626852 | EU626951 |
| Arecaceae | <i>Hyphaene coriacea</i> Gaertn. | OM236 | KNP | S25 03 08.3 E31 48 38.6 | 201 m | EU214271 | EU213778 | EU626853 | EU626952 |
| Arecaceae | <i>Hyphaene coriacea</i> Gaertn. | OM755 | KNP | S24 29 10.7 E31 48 29.4 | 259 m | EU214270 | EU213777 | EU626854 | EU626953 |
| Arecaceae | <i>Hyphaene petersiana</i> Klotzsch ex Mart | OM1296 | KNP | S22 38 18.4 E31 08 25.1 | 382 m | EU214272 | EU213779 | EU626855 | EU626954 |
| Arecaceae | <i>Hyphaene petersiana</i> Klotzsch ex Mart | OM908 | KNP | S22 32 55.9 E31 04 25.5 | 347 m | EU214273 | EU213780 | EU626856 | EU626955 |
| Myrothamnaceae | <i>Myrothamnus flabellifolia</i> Welw. | OM1137 | KNP | S25 06 15.4 E31 24 58.6 | 452 m | EU214275 | EU213840 | EU626857 | EU626956 |
| Myrothamnaceae | <i>Myrothamnus flabellifolia</i> Welw. | OM1209 | KNP | S25 04 03.5 E31 33 04.7 | 485 m | EU214276 | EU213841 | EU626858 | EU626957 |
| Myrothamnaceae | <i>Myrothamnus flabellifolia</i> Welw. | OM285 | KNP | S25 04 01.2 E31 33 04.8 | 577 m | EU214274 | EU213839 | EU626859 | EU626958 |
| Anacardiaceae | <i>Rhus gueinzii</i> Sond. | OM265 | KNP | S24 59 25.4 E31 27 19.6 | 268 m | EU214277 | EU213842 | EU626860 | EU626959 |
| Anacardiaceae | <i>Rhus gueinzii</i> Sond. | RL1366 | KNP | S25 17 23.1 E31 46 06.3 | 208 m | EU214278 | EU213843 | EU626861 | EU626960 |
| Anacardiaceae | <i>Rhus gueinzii</i> Sond. | RL1474 | KNP | S24 52 08.3 E31 45 22.4 | 283 m | EU214279 | EU213844 | EU626862 | EU626961 |
| Anacardiaceae | <i>Rhus leptodictya</i> Diels | RBN205 | KNP | S22 42 13.5 E30 57 56.4 | 487 m | EU214280 | EU213845 | EU626863 | EU626962 |
| Anacardiaceae | <i>Rhus leptodictya</i> Diels | RL1645 | KNP | S22 42 06.5 E30 58 10.5 | 499 m | EU214281 | EU213846 | EU626864 | EU626963 |
| Anacardiaceae | <i>Rhus leptodictya</i> Diels | RL1655 | KNP | S22 41 29.1 E31 01 38.4 | 448 m | EU214282 | EU213847 | EU626865 | EU626964 |
| Anacardiaceae | <i>Rhus transvaalensis</i> Engl. | OM282 | KNP | S25 08 53.2 E31 14 38.3 | 664 m | EU214283 | EU213848 | EU626866 | EU626965 |
| Anacardiaceae | <i>Rhus transvaalensis</i> Engl. | OM943 | KNP | S25 08 30.6 E31 14 07.8 | 610 m | - | EU213849 | EU626867 | EU626966 |
| Anacardiaceae | <i>Rhus transvaalensis</i> Engl. | RL1427 | KNP | S25 08 59.4 E31 14 35.0 | 630 m | EU214284 | EU213850 | EU626868 | EU626967 |
| Solanaceae | <i>Solanum panduriforme</i> Drège ex Dunal | OM1115 | KNP | S25 00 44.2 E31 27 13.7 | 341 m | EU214285 | EU213851 | EU626869 | EU626968 |
| Solanaceae | <i>Solanum panduriforme</i> Drège ex Dunal | OM326 | KNP | S25 04 18.8 E31 36 29.5 | 363 m | EU214286 | EU213852 | EU626870 | EU626969 |
| Solanaceae | <i>Solanum panduriforme</i> Drège ex Dunal | OM350 | KNP | S25 04 17.5 E31 36 29.2 | 354 m | EU214287 | EU213853 | EU626871 | EU626970 |
| Apiaceae | <i>Steganotaenia araliacea</i> Hochst. | OM1350 | KNP | S23 52 55.8 E31 15 00.9 | 422 m | EU214288 | EU213854 | EU626872 | EU626971 |
| Apiaceae | <i>Steganotaenia araliacea</i> Hochst. | OM1517 | KNP | S23 52 56.3 E31 15 06.4 | 420 m | EU214289 | EU213855 | EU626873 | EU626972 |
| Apiaceae | <i>Steganotaenia araliacea</i> Hochst. | OM566 | KNP | S25 04 36.8 E31 25 03.7 | 473 m | EU214290 | EU213856 | EU626874 | EU626973 |
| Orobanchaceae | <i>Striga elegans</i> Benth. | OM683 | KNP | S25 04 02.4 E31 33 06.1 | 383 m | EU214291 | - | EU626875 | EU626974 |

| Plant Family | name Checked on IPNI | Voucher | Location | GPS | Altitude | matK | trnH-psbA | atpF-atpH | psbK-psbI |
|--------------|--|---------|----------|-------------------------|----------|----------|-----------|-----------|-----------|
| Loganiaceae | <i>Strychnos decussata</i> (Pappe) Gilg | OM900 | KNP | S22 35 35.0 E31 06 37.5 | 329 m | EU214292 | EU213857 | EU626876 | EU626975 |
| Loganiaceae | <i>Strychnos decussata</i> (Pappe) Gilg | RL1560 | KNP | S23 24 53.0 E31 32 29.7 | 379 m | EU214293 | EU213858 | EU626877 | EU626976 |
| Loganiaceae | <i>Strychnos decussata</i> (Pappe) Gilg | RL1561 | KNP | S23 24 53.0 E31 32 29.7 | 379 m | EU214294 | EU213859 | EU626878 | EU626977 |
| Loganiaceae | <i>Strychnos madagascariensis</i> Spreng. ex Baker | RL1433 | KNP | S25 08 24.1 E31 14 51.5 | 641 m | EU214295 | EU213860 | EU626879 | EU626978 |
| Loganiaceae | <i>Strychnos madagascariensis</i> Spreng. ex Baker | RL1460 | KNP | S24 58 21.4 E31 23 21.8 | 342 m | EU214296 | EU213861 | EU626880 | EU626979 |
| Loganiaceae | <i>Strychnos madagascariensis</i> Spreng. ex Baker | RL1559 | KNP | S23 24 53.0 E31 32 29.7 | 379 m | EU214297 | EU213862 | EU626881 | EU626980 |
| Loganiaceae | <i>Strychnos spinosa</i> Lam. | OM220 | KNP | S24 59 49.9 E31 46 10.3 | 208 m | EU214298 | EU213863 | EU626882 | EU626981 |
| Loganiaceae | <i>Strychnos spinosa</i> Lam. | RL1346 | KNP | S25 04 51.2 E31 51 53.2 | 185 m | EU214299 | EU213864 | EU626883 | EU626982 |
| Loganiaceae | <i>Strychnos spinosa</i> Lam. | RL1652 | KNP | S22 39 39.3 E30 58 17.4 | 430 m | EU214300 | EU213865 | EU626884 | EU626983 |
| Loranthaceae | <i>Tapinanthus</i> Blume | OM825 | KNP | S22 59 46.4 E31 17 32.6 | 312 m | EU214301 | - | EU626885 | EU626984 |
| Velloziaceae | <i>Xerophyta retinervis</i> Baker | OM1213 | KNP | S25 08 32.4 E31 14 23.7 | 678 m | EU214302 | EU213866 | EU626886 | EU626985 |
| Velloziaceae | <i>Xerophyta retinervis</i> Baker | OM516 | KNP | S25 16 03.6 E31 47 53.3 | 267 m | EU214303 | EU213867 | EU626887 | EU626986 |
| Velloziaceae | <i>Xerophyta retinervis</i> Baker | OM562 | KNP | S25 04 36.8 E31 25 03.7 | 473 m | EU214304 | EU213868 | EU626888 | EU626987 |

Table 1. Material sampled for this study, species checked in IPNI, voucher, GPS and altitude information, GenBank accession numbers. All vouchers have been collected in triplicate, one for Kew Herbarium, one for the herbarium of the KNP at Skukuza (South Africa), and one for the National Herbarium at Pretoria (South Africa).

Genetic analyses. Inter- and intra-specific genetic divergences were calculated using each potential DNA barcode following Meyer and Paulay . Three different metrics were used to characterize intra-specific divergence: (i) average pairwise distances between all individuals sampled within those species that had at least two representatives, (ii) ‘mean theta’, with theta being the average pairwise distances calculated for each species that had more than one representative, thereby eliminating biases associated with uneven sampling among taxa and (iii) average coalescent depth, i.e. the depth of a node linking all sampled extant members of a species, ‘book-ending’ intra-specific variability. Genetic distances between con-generic species were used to characterize inter-specific divergence. For each barcode, pairwise distances were calculated with the simplest K2P model following Lahaye et al. in which this model showed the best results. This model also utilizes the CBOL advises for distance calculations (barcoding.si.edu/). Wilcoxon Signed Rank Tests were performed to compare intra- and inter-specific variability for every pair of barcodes following Kress and Erickson . We evaluated ‘DNA barcoding gaps’ by comparing the distribution of intra- versus inter-specific divergences. Median and Wilcoxon Two-Sample Tests were used to evaluate whether these distributions overlapped.

Phylogenetic analyzes. To evaluate whether species were recovered as monophyletic with each barcode, we used standard phylogenetic techniques. Note that this is not to say that barcodes can be used to reconstruct phylogenies, because in this case we are disregarding the recovered inter-specific relationships. Trees were built with PAUP4b10* using Maximum Parsimony (MP) and UPGMA, the two best algorithms in terms of percentages of species correctly identified . UPGMA trees were inferred with PAUP4b10* from K2P distances. MP analyses were performed using tree bisection-reconnection (TBR), branch swapping and 1,000 random addition sequence replicates keeping 10 trees at each step. MP analyses have been performed with and without coding

indels as a 5th state in order to assess the impact of keeping this information for barcoding purposes.

Coalescence analyses. For each barcode, we identified those clusters that were derived from an independent coalescence process and asked whether they matched previously recognized taxonomic species, using methods developed by Pons et al. and Fontaneto et al. . The likelihood of waiting times between successive branching events on a DNA barcode-based tree was calculated under the null model that all terminals were derived from a single coalescence process, and under the alternative model that all taxa derived from a set of two independently evolving populations. With the alternative model, a threshold age T was calculated, at which point the older nodes represented inter-specific diversification events whereas the younger nodes represented separate coalescent processes typical of intra-specific clusters. We used DNA barcode-based trees from MP and transformed branch lengths with nonparametric rate smoothing to produce ultrametric trees, i.e. branch lengths reflecting time only. We also used the ultrametric UPGMA trees. Likelihood models were determined using an R script available from TGB.

Results & Discussion

Molecular characteristics and PCR success. Amplification was generally successful for each potential barcode tested with more than 92% of taxa successfully amplified and sequenced (Table 2). The best percentage was given by *matK* with 99% of taxa sequenced and the lowest percentage was obtained for *trnH-psbA* with 92%. The potential DNA barcode *psbK-psbI* showed PCR and sequencing performances very close to those of *matK* with 98% of taxa successfully amplified. Both *atpF-atpH* and *trnH-psbA* failed to amplify the parasitic/non-chlorophytic plant *Hydnora johanis*. Alignment of sequences was unproblematic for *matK* and *psbK-psbI*, but *trnH-psbA* and *atpF-atpH*

presented significant difficulties due to a high level of length variation (225 to 758 bp and 218 to 847 bp, respectively). Because its alignment was not reliable by Clustal X, we performed a first visual alignment between congeneric species and then aligned all taxa by adding as many gaps as necessary to keep the homology between congeneric species for inter- and intraspecific calculations. The alignment of *trnH-psbA* revealed a highly conservative intron only for the Orchidaceae and Amaryllidaceae which has been identified previously . Combining *matK* to one of the other potential barcodes allowed building a matrix including sequences for all taxa (Table 2).

| | |
|---------------------------------|-------|
| <i>matK</i> | 99% |
| <i>psbK-psbI</i> | 98% |
| <i>trnH-psbA</i> | 92.1% |
| <i>atpF-atpH</i> | 93.1% |
| <i>matK+trnH-psbA</i> | 100% |
| <i>matK+trnH-psbA+atpF-atpH</i> | 100% |
| <i>matK+trnH-psbA+psbK-psbI</i> | 100% |
| <i>matK+atpF-atpH</i> | 100% |
| <i>matK+psbK-psbI</i> | 100% |
| <i>matK+atpF-atpH+psbK-psbI</i> | 100% |
| <i>4 loci</i> | 100% |

Table 2. Percentages of taxa represented in each matrix by at least one sequence.

Intra- and Inter-specific diversities. Performances of each DNA barcode was assessed by means of inter- and intra-specific diversity calculated from K2P (Kimura's two parameters) pairwise distance matrices (barcoding.si.edu/; Table 3). The highest inter-specific diversity was reached by *atpF-atpH* (3.45%) followed by *trnH-psbA* (2.55%) and the lowest was given by *psbK-psbI* (1.06%) with *matK* between these (1.34%). Regarding

the different metrics to infer the intra-specific differences, the mean theta was in most cases similar to the average of overall intra-specific distances because there is no bias associated with species over-sampled in our study with the majority of the species represented by three specimens. The mean coalescent depth was slightly superior to the average of overall interspecific distances because it takes into consideration only the highest distance between specimens sampled for a species. Results showed the highest mean of intraspecific differences for *trnH-psbA* regardless of the metric used (Table 3). The lowest values were obtained for both *atpF-atpH* and *psbK-psbI*. Wilcoxon rank tests performed on the different distance matrices showed with very high significance that *trnH-psbA* had by far the highest inter-specific variability, followed by *matK* and *atpF-atpH*, which had a similar divergence (Table 4). The highest intra-specific distances were also significantly reached by *trnH-psbA* whereas the three other loci presented almost similar values (Table 5).

| | matK | trnH- psbA | atpF- atpH | psbK- psbl | 4 loci | matK+ trnH- psbA | matK+atpF- atpH+trnH- psbA | matK+psbK- psbl+trnH- psbA | matK+ atpF- atpH | matK+ psbK- psbl | matK+psbK- psbl+ atpF-atpH |
|--|--------|---------------|---------------|---------------|--------|------------------------|----------------------------------|----------------------------------|------------------------|------------------------|----------------------------------|
| Mean of all interspecific distances | 0.0134 | 0.0255 | 0.0345 | 0.0106 | 0.0172 | 0.0175 | 0.0189 | 0.0157 | 0.0168 | 0.0118 | 0.0150 |
| St. deviation +/- | 0.0127 | 0.0227 | 0.0665 | 0.0096 | 0.0151 | 0.0154 | 0.0180 | 0.0121 | 0.0201 | 0.0092 | 0.0159 |
| Mean of all intraspecific distances | 0.0012 | 0.0017 | 0.0004 | 0.0005 | 0.0009 | 0.0012 | 0.0009 | 0.0011 | 0.0007 | 0.0009 | 0.0007 |
| St. deviation +/- | 0.0040 | 0.0041 | 0.0015 | 0.0012 | 0.0015 | 0.0026 | 0.0017 | 0.0021 | 0.0020 | 0.0026 | 0.0016 |
| Mean Theta | 0.0012 | 0.0015 | 0.0007 | 0.0005 | 0.0008 | 0.0012 | 0.0009 | 0.0010 | 0.0007 | 0.0009 | 0.0007 |
| St. deviation +/- | 0.0037 | 0.0032 | 0.0023 | 0.0010 | 0.0013 | 0.0023 | 0.0015 | 0.0018 | 0.0018 | 0.0024 | 0.0015 |
| Mean coalescent depth | 0.0017 | 0.0023 | 0.0008 | 0.0008 | 0.0013 | 0.0017 | 0.0014 | 0.0016 | 0.0012 | 0.0013 | 0.0011 |
| St. deviation +/- | 0.0050 | 0.0047 | 0.0023 | 0.0016 | 0.0018 | 0.0032 | 0.0021 | 0.0026 | 0.0026 | 0.0033 | 0.0021 |
| Number of measurements for all intraspecific distances | 93 | 90 | 84 | 91 | 95 | 95 | 95 | 95 | 95 | 95 | 95 |
| Number of measurements for all interspecific distances | 200 | 194 | 168 | 194 | 206 | 206 | 206 | 206 | 206 | 206 | 206 |

Table 3. Measures of inter- and intra-specific K2P distances for four potential barcodes and different combinations applied to a selective sampling from the KNP.

| Wilcoxon Signed-Ranks Test – Interspecific pair-distances | | |
|--|--|---|
| matK vs trnH-psbA | W+ = 1462, W- = 14648, N = 179, p <= 2.216e-21 | matK << trnH-psbA |
| matK vs atpF-atpH | W+ = 4977, W- = 5608, N = 145, p <= 0.5341 | matK = atpF-atpH |
| matK vs psbK-psbl | W+ = 8655, W- = 6051, N = 171, p <= 0.0447 | matK > psbK-psbl |
| trnH-psbA vs atpF-atpH | W+ = 8482, W- = 3608, N = 155, p <= 1.345e-05 | trnH-psbA > atpF-atpH |
| trnH-psbA vs psbK-psbl | W+ = 13538, W- = 2572, N = 179, p <= 2.88e-15 | trnH-psbA >> psbK-psbl |
| atpF-atpH vs psbK-psbl | W+ = 7663, W- = 2922, N = 145, p <= 2.902e-06 | atpF-atpH > psbK-psbl |
| 4 loci vs matK+trnH-psbA | W+ = 7286, W- = 12217, N = 197, p <= 0.002095 | 4 loci < matK+trnH-psbA |
| 4 loci vs matK+trnH-psbA+atpF-atpH | W+ = 5244, W- = 14259, N = 197, p <= 1.859e-08 | 4 loci < matK+trnH-psbA+atpF-atpH |
| 4 loci vs matK+trnH-psbA+psbK-psbl | W+ = 6661, W- = 12060, N = 193, p <= 0.0005137 | 4 loci < matK+trnH-psbA+psbK-psbl |
| 4 loci vs matK+atpF-atpH | W+ = 14310, W- = 5193, N = 197, p <= 1.284e-08 | 4 loci > matK+atpF-atpH |
| 4 loci vs matK+psbK-psbl | W+ = 15830, W- = 3673, N = 197, p <= 3.333e-14 | 4 loci > matK+psbK-psbl |
| 4 loci vs matK+psbK-psbl+atpF-atpH | W+ = 15351, W- = 4152, N = 197, p <= 2.807e-12 | 4 loci < matK+atpF-atpH+psbK-psbl |
| matK+trnH-psbA vs matK+trnH-psbA+atpF-atpH | W+ = 12287, W- = 6434, N = 193, p <= 0.0001661 | matK+trnH-psbA > matK+trnH-psbA+atpF-atpH |
| | | matK+trnH-psbA > matK+trnH-psbA+psbK-psbl |
| matK+trnH-psbA vs matK+trnH-psbA+psbK-psbl | W+ = 13374, W- = 6129, N = 197, p <= 6.174e-06 | matK+trnH-psbA > matK+trnH-psbA+psbK-psbl |
| matK+trnH-psbA vs matK+atpF-atpH | W+ = 13379, W- = 6124, N = 197, p <= 5.995e-06 | matK+trnH-psbA > matK+atpF-atpH |
| matK+trnH-psbA vs matK+psbK-psbl | W+ = 16218, W- = 3285, N = 197, p <= 7.1e-16 | matK+trnH-psbA >> matK+psbK-psbl |
| | | matK+trnH-psbA > matK+atpF-atpH+psbK-psbl |
| matK+trnH-psbA vs matK+atpF-atpH+psbK-psbl | W+ = 13179, W- = 6324, N = 197, p <= 1.894e-05 | psbl |

Table 4. Wilcoxon signed rank tests of inter-specific divergence among loci.

| Wilcoxon Signed-Ranks Test - Intraspecific pair-distances | | |
|--|---|---|
| matK vs trnH-psbA | W+ = 298, W- = 605, N = 42, p <= 0.05574 | matK < trnH-psbA |
| matK vs atpF-atpH | W+ = 334, W- = 162, N = 31, p <= 0.09384 | matK = atpF-atpH |
| matK vs psbK-psbl | W+ = 299, W- = 229, N = 32, p <= 0.5189 | matK = psbK-psbl |
| trnH-psbA vs atpF-atpH | W+ = 340, W- = 95, N = 29, p <= 0.008339 | trnH-psbA > atpF-atpH |
| trnH-psbA vs psbK-psbl | W+ = 375, W- = 121, N = 31, p <= 0.01318 | trnH-psbA > psbK-psbl |
| atpF-atpH vs psbK-psbl | W+ = 89, W- = 142, N = 21, p <= 0.3662 | atpF-atpH = psbK-psbl |
| 4 loci vs matK+trnH-psbA | W+ = 450, W- = 981, N = 53, p <= 0.01898 | 4 loci < matK+trnH-psbA |
| 4 loci vs matK+trnH-psbA+atpF-atpH | W+ = 486, W- = 945, N = 53, p <= 0.04263 | 4 loci < matK+trnH-psbA+atpF-atpH |
| | W+ = 319, W- = 1007, N = 51, p <= | |
| 4 loci vs matK+trnH-psbA+psbK-psbl | 0.001283 | 4 loci < matK+trnH-psbA+psbK-psbl |
| 4 loci vs matK+atpF-atpH | W+ = 923, W- = 508, N = 53, p <= 0.06687 | 4 loci = matK+atpF-atpH |
| 4 loci vs matK+psbK-psbl | W+ = 901, W- = 530, N = 53, p <= 0.1015 | 4 loci = matK+psbK-psbl |
| 4 loci vs matK+psbK-psbl+atpF-atpH | W+ = 906, W- = 525, N = 53, p <= 0.09256 | 4 loci = matK+atpF-atpH+psbK-psbl |
| matK+trnH-psbA vs matK+trnH-psbA+atpF-atpH | W+ = 810, W- = 271, N = 46, p <= 0.003294 | matK+trnH-psbA > matK+trnH-psbA+atpF-atpH |
| | | matK+trnH-psbA > matK+trnH-psbA+psbK-psbl |
| matK+trnH-psbA vs matK+trnH-psbA+psbK-psbl | W+ = 833, W- = 392, N = 49, p <= 0.02864 | |
| | W+ = 924, W- = 252, N = 48, p <= | |
| matK+trnH-psbA vs matK+atpF-atpH | 0.0005795 | matK+trnH-psbA > matK+atpF-atpH |
| matK+trnH-psbA vs matK+psbK-psbl | W+ = 854, W- = 371, N = 49, p <= 0.01652 | matK+trnH-psbA > matK+psbK-psbl |
| | W+ = 1068, W- = 363, N = 53, p <= | matK+trnH-psbA > matK+atpF-atpH+psbK-psbl |
| matK+trnH-psbA vs matK+atpF-atpH+psbK-psbl | 0.001832 | psbl |

Table 5. Wilcoxon signed rank tests of intra-specific difference among loci.

In a multi loci approach for DNA barcoding purposes, the highest mean of inter-specific variability was achieved by *matK* combined with *trnH-psbA* and *atpF-atpH* whereas the highest mean of intra-specific distances were given by combining *matK* with *trnH-psbA* (Table 3). Wilcoxon statistical rank tests showed the combination *matK* + *trnH-psbA* having the highest inter-specific pair-distances (Table 4). They revealed also that all the combinations including *trnH-psbA* had a higher intra-specific variability than combinations without it (Table 5).

Distribution of distances. Accuracy of each DNA barcode was assessed by looking at the distribution of inter- and intraspecific K2P distances to infer the barcoding gap . Distributions were similar for each single potential barcode with two peaks of inter- and intraspecific variability that could be distinguished (Figure 2).

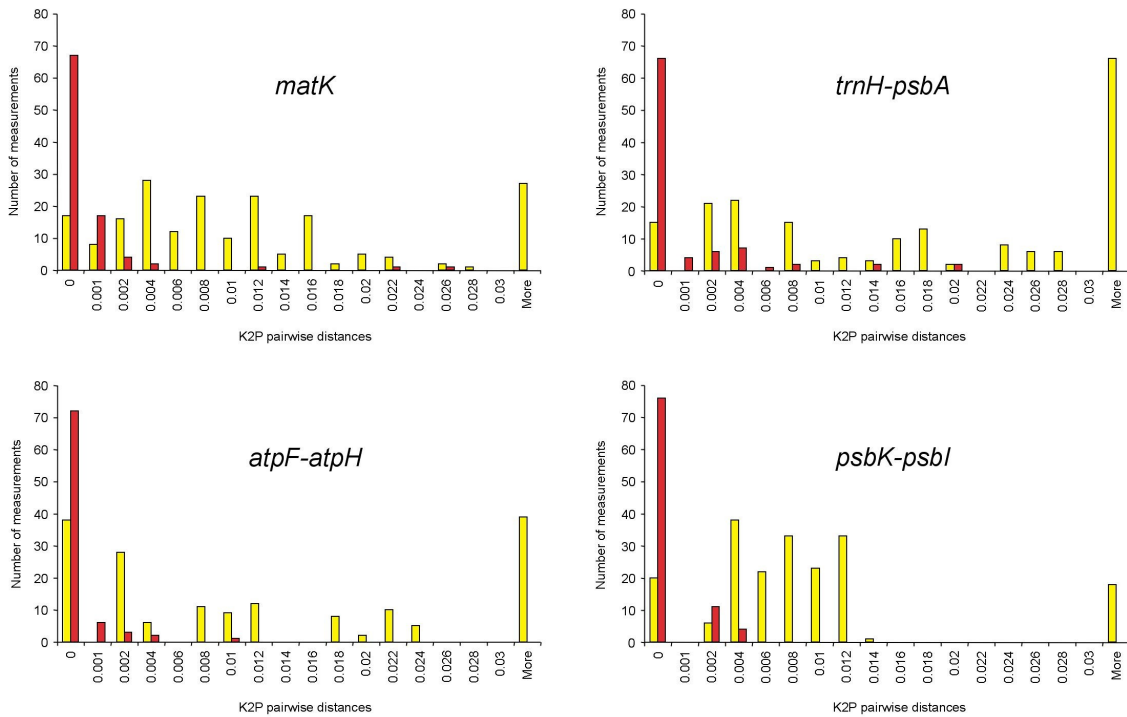


Figure 2. Relative distributions of inter-specific divergence between con-generic species (yellow) and intra-specific K2P distances (red) for four single loci: *matK*, *trnH-psbA*, *psbK-psbI* and *atpF-*

atpH. Barcoding gaps were assessed with Median tests and Wilcoxon Two-Sample tests, and all were highly significant ($p < 0.0001$).

Each distribution also showed a slight overlap between intra- and inter-specific distances, but to a lesser extent for *matK* and *trnH-psbA*. Combining the different loci showed distributions with a slight decrease of this overlap (Figure 3).

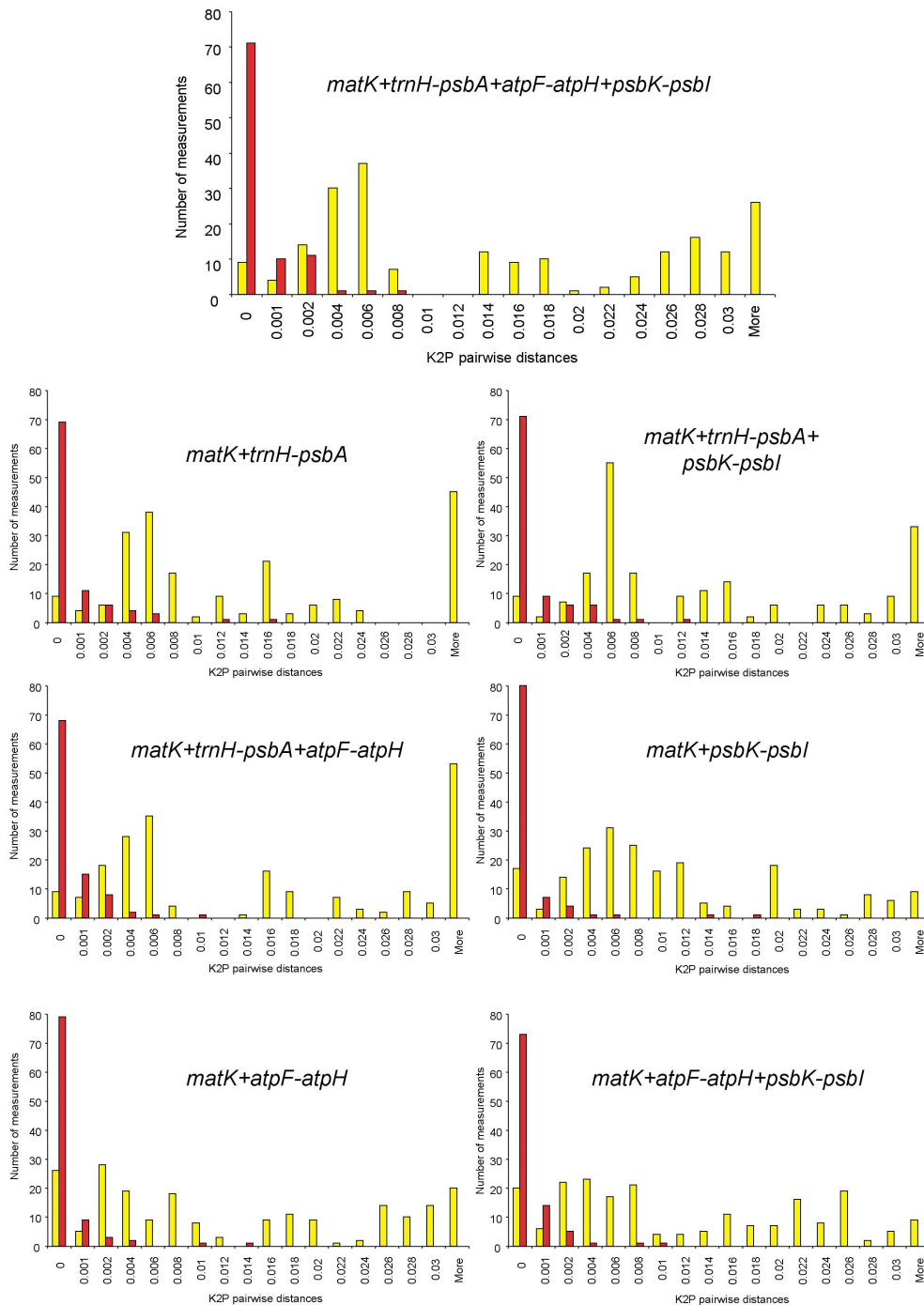


Figure 3. Relative distributions of inter-specific divergence between con-generic species (yellow) and intra-specific K2P distances (red) for 7 different combinations keeping *matK* for each.

Barcoding gaps were assessed with Median tests and Wilcoxon Two-Sample tests, and all were highly significant ($p < 0.0001$).

Two clear peaks were still distinguishable and a slight overlap still occurred between low classes of intra- and inter-specific distances, but the overlap observed was less than that

for the single locus approach. These observations were confirmed by median and Wilcoxon two samples statistical tests differentiating the medians for the former and the medians plus the distributions between the inter- and intra-specific distances for the latter. For each distribution, Median and Wilcoxon two sample tests were significant (Table 6). In a single locus approach, the highest significances were given by *matK* and *psbK-psbI*. Combining the loci made the significance increasing with the highest significance given by the combination *matK+trnH-psbA+psbK-psbI*.

| K2P distributions | median test | Wilcoxon Two Sample Test |
|---------------------------------|---|--|
| <i>matK</i> | #A = 199 #B = 93, Median = 0.00524, p <= 1.11e-26 | #A = 200 #B = 93, W = 6020.5, p <= 9.314e-30 |
| <i>trnH-psbA</i> | #A = 194 #B = 90, Median = 0.00799, p <= 1.11e-22 | #A = 194 #B = 90, W = 5634, p <= 6.125e-29 |
| <i>atpF-atpH</i> | #A = 168 #B = 84, Median = 0.00216, p <= 1.52e-23 | #A = 168 #B = 84, W = 5526, p <= 8.996e-21 |
| <i>psbK-psbI</i> | #A = 194 #B = 91, Median = 0.00509, p <= 1.44e-29 | #A = 194 #B = 91, W = 5333, p <= 2.524e-32 |
| 4 loci | #A = 206 #B = 95, Median = 0.00608, p <= 1.23e-28 | #A = 206 #B = 95, W = 5507, p <= 2.394e-36 |
| <i>matK+trnH-psbA</i> | #A = 206 #B = 95, Median = 0.00648, p <= 8.07e-28 | #A = 206 #B = 95, W = 5675, p <= 4.825e-35 |
| <i>matK+trnH-psbA+atpF-atpH</i> | #A = 206 #B = 95, Median = 0.00574, p <= 5.11e-29 | #A = 206 #B = 95, W = 5642.5, p <= 2.711e-35 |
| <i>matK+trnH-psbA+psbK-psbI</i> | #A = 206 #B = 95, Median = 0.00676, p <= 5.11e-29 | #A = 206 #B = 95, W = 5540, p <= 4.338e-36 |
| <i>matK+atpF-atpH</i> | #A = 206 #B = 95, Median = 0.00401, p <= 1.2e-26 | #A = 206 #B = 95, W = 6318, p <= 2.802e-30 |
| <i>matK+psbK-psbI</i> | #A = 206 #B = 95, Median = 0.00607, p <= 8.07e-28 | #A = 206 #B = 95, W = 6064, p <= 4.064e-32 |
| <i>matK+atpF-atpH+psbK-psbI</i> | #A = 206 #B = 95, Median = 0.00493, p <= 2.92e-28 | #A = 206 #B = 95, W = 6026.5, p <= 2.151e-32 |

Table 6. Median and Wilcoxon two sample statistical tests applied to the distributions of intra- and inter-specific K2P distances for each potential DNA barcode.

Species identification. The performance of each DNA barcode in identifying and delineating species was assessed by the percentage of monophyletic species recovered by MP and UPGMA analyses (Table 7). Because *trnH-psbA* and *atpF-atpH* were highly variable and their alignment showed many indels, MP analyses were performed with and without coding the gaps as 5th state to infer whether this information could be useful for barcoding purposes. The highest values of species monophyly were obtained from UPGMA reconstruction. The UPGMA analysis of *trnH-psbA* gave 90.3% of species monophyletic but only 77.4% supported by BS>50%. Although *matK* and *psbK-psbI*

grouped 87.5% of the species under UPGMA reconstruction, they gave 78.1% of monophyletic species with a BS>50%, a value higher than *trnH-psbA*. *MatK* showed the best percentage of species correctly identified using MP reconstruction. Coding the gaps as 5th state in the MP analysis did not significantly affect the results obtained for *matK* and *psbK-psbI*, but it increased the percentages of species correctly identified by 6% and 7% given by the more variable *atpF-atpH* and *trnH-psbA*, respectively. In a multi-loci approach, it is noteworthy that combining all potential barcodes did not result in 100% monophyly for species whatever the reconstruction method. Each barcode failed in grouping the two different species of *Faurea*. That can be done by using the intergenic locus *atpF-atpH* and by coding the gaps in the matrix as 5th state of character, but this decreases the total percentage of monophyletic species. In a multi-loci approach, combining *matK* and *psbK-psbI* gave the highest percentage of monophyletic species (Table 7).

| | UPGMA | MP | MP+5th state character |
|---|-------------|-------------|------------------------|
| <i>trnH-psbA</i> | 90.3 (77.4) | 71 (71) | 77.4 (74.2) |
| <i>matK</i> | 87.5 (78.1) | 75 (75) | 75 (75) |
| <i>psbK-psbI</i> | 87.5 (78.1) | 62.5 (68.8) | 53.1 (53.1) |
| <i>atpF-atpH</i> | 82.8 (69) | 65.5 (65.5) | 72.4 (69) |
| <i>matK+psbK-psbI</i> | 93.8 (87.5) | 81.3 (81.3) | 59.4 (56.3) |
| <i>matK+trnH-psbA+psbK-psbI</i> | 93.5 (90.3) | 87.1 (87.1) | 80.6 (80.6) |
| <i>matK+atpF-atpH+psbK-psbI</i> | 93.1 (86.2) | 86.2 (86.2) | 82.8 (82.8) |
| <i>matK+trnH-psbA+atpF-atpH+psbK-psbI</i> | 92.9 (89.3) | 85.7 (85.7) | 82.1 (82.1) |
| <i>matK+trnH-psbA</i> | 90.3 (87.1) | 83.9 (83.9) | 77.4 (77.4) |
| <i>matK+atpF-atpH</i> | 89.7 (82.8) | 79.3 (79.3) | 79.3 (79.3) |
| <i>matK+trnH-psbA+atpF-atpH</i> | 89.3 (85.7) | 82.1 (82.1) | 82.1 (82.1) |

Table 7. Proportion (%) of monophyletic species (with BS > 50% in brackets) recovered with UPGMA and MP analyses with gaps not coded and coded as a fifth character state.

Coalescence. The accuracy of the DNA barcode can be assessed by evaluating the ability of each candidate to give genetic clusters that are derived from an independent coalescence process and that corresponds to a recognized taxonomic species . The highest number of genetic clusters corresponding to taxonomic species was given using the UPGMA trees. Transforming MP trees by NPRS for coalescence analysis gave half the genetic clusters corresponding to taxonomic species compared to the UPGMA trees (Table 7). In a single barcode approach, *matK* gave the highest numbers of genetic clusters corresponding to taxonomic species (Table 8). When *matK* was combined with *psbK-psbI* the value increased from 22 to 23 genetic clusters corresponding to recognized species. Molecular evolutionary rates of both *matK* and *psbK-psbI* showed higher abilities to differentiate independently evolving entities corresponding to taxonomic species than the high variable *trnH-psbA* and *atpF-atpH*.

| | UPGMA | MP | Nos. of potential genetic clusters |
|---|-------|----|------------------------------------|
| <i>matK</i> | 22 | 11 | 32 |
| <i>psbK-psbI</i> | 20 | 15 | 32 |
| <i>atpF-atpH</i> | 18 | 12 | 29 |
| <i>trnH-psbA</i> | 16 | 12 | 31 |
| <i>matK+psbK-psbI</i> | 23 | 8 | 32 |
| <i>matK+atpF-atpH+psbK-psbI</i> | 20 | 4 | 29 |
| <i>matK+atpF-atpH</i> | 20 | 6 | 29 |
| <i>matK+trnH-psbA+psbK-psbI</i> | 3 | 7 | 31 |
| <i>matK+trnH-psbA+atpF-atpH+psbK-psbI</i> | | | |
| <i>psbI</i> | 3 | 1 | 28 |
| <i>matK+trnH-psbA</i> | 3 | 8 | 31 |
| <i>matK+trnH-psbA+atpF-atpH</i> | 3 | 5 | 28 |

Table 8. Coalescence analyses indicating the number of independent genetic clusters corresponding to taxonomically recognized species.

Our results showed that combining *matK* to *trnH-psbA* and *psb-psbI* can slightly increase its performance in identifying species. However we still support the conclusion of Lahaye et al. , i.e. that *matK* should be used for DNA barcoding of plants in a single locus approach and that case-by-case additional barcodes are developed for problematic groups.

Literature Cited